RECENT EXPERIENCE WITH HIGH-LUMINOSITY OPERATION OF SuperKEKB

Y. Ohnishi*, High Energy Accelerator Research Organization (KEK), Tsukuba, Japan
on behalf of the SuperKEKB team

Abstract

SuperKEKB is a positron-electron collider employing the nano-beam scheme which enable an extremely low beta function at the interaction point (IP) compared to the bunch length. The vertical beta function at the IP is less than 1 mm, the smallest among all existing and previous colliders. We discuss recent results on beam-beam interactions and the performance of the crab-waist scheme, which enhances luminosity. Sudden beam loss, which cannot be explained by conventional beam dynamics, and the nonlinear collimator – a key device for reducing both beam background and impedance – are also highlighted as crucial issues. This paper presents recent machine operation results and performance achievements of SuperKEKB, which provide insight into the design of future high-energy and high-luminosity colliders.

INTRODUCTION

The luminosity for e^+e^- colliders is expressed by

$$L = \frac{N_+ N_- n_b f_0}{2\pi\sqrt{\sigma_{x+}^{*2} + \sigma_{x-}^{*2}}\sqrt{\sigma_{y+}^{*2} + \sigma_{y-}^{*2}}} R_L, \tag{1}$$

where $N_\pm$ is the bunch population for positrons or electrons, n_b is the number of bunches, f_0 is the revolution frequency, $\sigma_{x,y}^*$ is the transverse beam size at the interaction point (IP), and R_L is the luminosity reduction factor due to the geometrical loss such as an hourglass and a crossing angle effects.

For flat beams, achieving a vertical beam size σ_y^* in the range of 30-50 nm is typically a design goal for high-luminosity colliders [1]. This implies that both the vertical beta function at the IP, β_y^*, and the vertical emittance, ε_y, must be below 1 mm and 10 pm, respectively. The hourglass requirement to reduce the luminosity reduction is

$$\beta_y^* > \frac{\sigma_z}{\sqrt{1+\Phi^2}}, \tag{2}$$

where Φ is the Piwinski angle defined by

$$\Phi = \frac{\sigma_z}{\sigma_x^*}\tan\frac{\theta_c}{2}, \tag{3}$$

σ_z is the bunch length, and θ_c is the crossing angle. However, it is difficult to shorten σ_z to less than 1 mm. To overcome the hourglass effect, a large Piwinski angle is required, which implies a large crossing angle and a low emittance. This approach is known as the nano-beam scheme. In the case of SuperKEKB, Φ is approximately 12 with the current machine parameters, and σ_z is typically about 6 mm. Accordingly, β_y^* can, in principle, be squeezed down to 0.5 mm.

In the nano-beam scheme, the luminosity reduction becomes

$$R_L = \left(1 + \frac{\sigma_{z+}^2 + \sigma_{z-}^2}{\sigma_{x+}^{*2} + \sigma_{x-}^{*2}}\tan^2\frac{\theta_c}{2}\right)^{-1/2} R_H, \tag{4}$$

where R_H is the another luminosity reduction factor, which can be approximated to be 1. The luminosity formula is modified by using Eq.(4):

$$L = \frac{N_+ N_- n_b f_0}{\pi\theta_c\sqrt{\sigma_{z+}^2 + \sigma_{z-}^2}\sqrt{\sigma_{y+}^{*2} + \sigma_{y-}^{*2}}}. \tag{5}$$

The horizontal beam size at the IP, σ_x^* does not affect the luminosity explicitly.

On the other hand, the vertical beam-beam parameter is written by

$$\xi_{y\pm} = \frac{r_e}{\pi\gamma_\pm}\frac{\beta_{y\pm}^* N_\mp}{\theta_c\sigma_{z\pm}\sigma_{y\mp}^*} \propto N_\mp\sqrt{\frac{\beta_y^*}{\varepsilon_{y\mp}}}, \tag{6}$$

where $\gamma_\pm$ is the Lorentz factor. If β_y^* is the same value between two rings, ξ_y is proportional to square root of the ratio of β_y^* to ε_y. If the ratio can be constant, the luminosity increases as squeezing β_y^* and decreasing ε_y with keeping constant ξ_y.

Two advanced technologies have been adopted in the recent colliders: the nano-beam scheme, as described in the previous section, and the crab-waist scheme [2]. To implement the crab-waist scheme, a Hamiltonian of the form $H_{cw} = (1/2\tan\theta_c)x^* p_y^{*2}$ is introduced at the IP. The sextupoles located on both sides of the IP are employed to shift the vertical waist along the beam axis in response to the horizontal beam position. The phase advance between each crab-waist sextupole and the IP is adjusted to be $n\pi$ in the horizontal plane and $(m+1/2)\pi$ in the vertical place.

At SuperKEKB, the sextupoles used for the local chromaticity correction can also function as the crab-waist sextupoles [3]. The lattice design of the interaction region (IR) in the LER is shown in Fig. 1. The lattice design in the HER is similar to that of the LER. Two sextupoles are connected by $-I'$ transformation and the vertical phase advance between the first sextupole and the IP is almost $3\pi/2$ and π in the horizontal plane. Their magnetic field strength, k values are

$$K_2^{(1,2)} = K_2 \mp K_{2,cw}/2, \tag{7}$$

where

$$K_{2,cw} = \frac{R_{cw}}{\tan\theta_c}\frac{1}{\beta_y^s\beta_y^*}\sqrt{\frac{\beta_x^*}{\beta_x^s}}, \tag{8}$$

* yukiyoshi.onishi@kek.jp

R_{cw} is the crab-waist ratio, $\beta^s_{x,y}$ is the beta functions at the sextupoles. The R_{cw} for the LER is 80 % and 40 % or 60 % is used for the HER, respectively. The betatron resonances related to beam-beam interactions can be suppressed by the crab-waist scheme [4, 5].

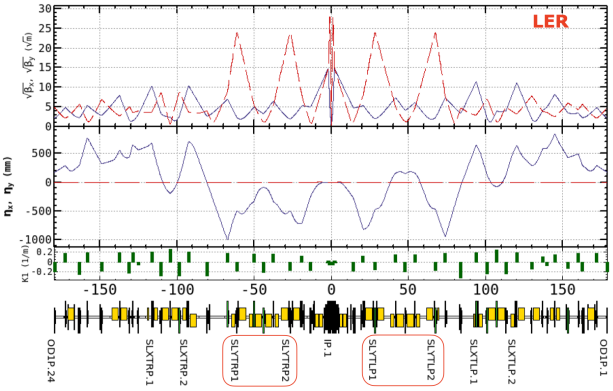

Figure 1: Lattice design of the interaction region (IR) in the LER. Two pairs of crab-waist sextupoles are indicated by the red rectangles.

BEAM-BEAM PERFORMANCE

The specific luminosity is defined by

$$L_{sp} = \frac{L}{n_b I_{b+} I_{b-}} \propto \frac{1}{\sqrt{\sigma^2_{z+} + \sigma^2_{z-}}\sqrt{\sigma^{*2}_{y+} + \sigma^{*2}_{y-}}}, \qquad (9)$$

where I_b is the bunch current. Figure 2 shows the specific luminosity as a function of the bunch current product. The β^*_y is 1 mm for the both rings, β^*_x is 80 mm in the LER and 60 mm in the HER, respectively. The beam-beam experiment was performed under the condition of 393 bunches without the crab-waist and with the crab-waist, 80 % in the LER and 40 % in the HER. In the case of the specific luminosity without the crab-waist, two vertical tunes, $\nu_y = 46.59$ and $\nu_y = 46.567$ were tested in the LER. The lower vertical tune is a better performance because it is far from the betatron resonance related to beam-beam interactions such as $\nu_x + 4\nu_y + \alpha = N$ [6]. The specific luminosity with the crab-waist scheme is higher than without it, especially at higher bunch current products [7]. This is because the crab-waist scheme further suppresses the strength of beam-beam resonances.

The beam-beam blowup has been observed, and the specific luminosity decreases gradually as the bunch current product increases. Beam-Beam simulations using the Strong-Strong model (BBSS) [8] predict no beam-beam blowup up to 0.2 mA^2 for the ideal case with the crab-waist scheme. However, experiments show a luminosity about 30 % lower than the ideal simulation case at a bunch current product of 0.4 mA^2. To understand the luminosity degradation at higher bunch products, combined effects of beam-beam interactions, lattice nonlinear, and impedance effects must be considered.

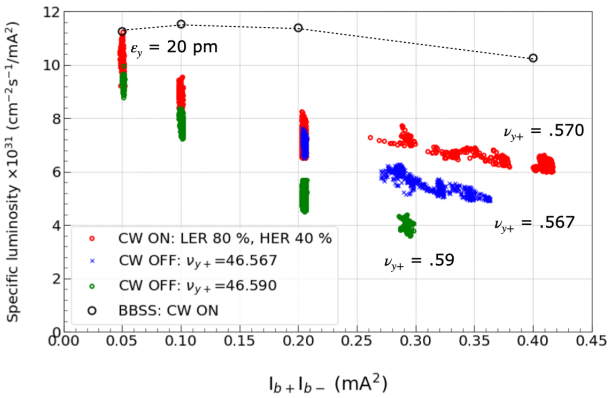

Figure 2: Specific luminosity with crab waist and without crab waist scheme. Number of bunches is 393.

Figures 3 and 4 show the luminosity runs for $\beta^*_y = 1$ mm. The number of bunches is 2346. The β^*_x is 60 mm in the HER in the both figures, and β^*_x in the LER is 80 mm in Fig. 3 and 60 mm in Fig. 4. The horizontal and vertical emittance are measured by the X-ray beam size monitor (XRM) with assuming the nominal beta functions. The horizontal emittance blowup in the LER and flip-flop behavior for the vertical emittance were observed at $\beta^*_x = 80$ mm in the LER. Moreover, the beam injection became more difficult at higher bunch current product due to beam-beam interactions. The horizontal tune close to the synchro-beta resonance helps the beam injection. The horizontal emittance remained stable after squeezing β^*_x from 80 mm to 60 mm. A coherent X-Z beam-beam instability is one of the candidates and the lower β^*_x mitigates the coherent X-Z beam-beam instability.

SUDDEN BEAM LOSS

We have observed that large beam loss occurs suddenly with in a few turns, without significant coherent beam oscillations [9]. This phenomenon is referred to as "Sudden Beam Loss (SBL)". SBL events could result in serious consequences such as damage to the collimator head, quench of the final focus superconducting magnets, and damage to the Belle II detector. The coherent orbit deviation is a few hundred μm measured by the bunch oscillation recorder (BOR) [10]. A large fraction of the storage beam is lost before the beam abort as shown in Fig. 5. No clear threshold has been observed in beam current or bunch current for SBL events. Vacuum pressure bursts have also been observed, and most of the SBL events in the LER have occurred at specific locations, such as the wiggler section [11].

Black color stains were observed inside the vacuum pipe during inspection. In particular, many black stains were observed around the MO-type flange in the wiggler section of the LER. The vacuum sealant VACSEAL had been applied to the MO-type flange to prevent vacuum leakage (see Fig. 6). Since VACSEAL is not originally black in color, the observed black stains are likely the result of exposure to intense synchrotron radiation (SR). Spectroscopic analysis confirmed that the stains consist of amorphous graphite.

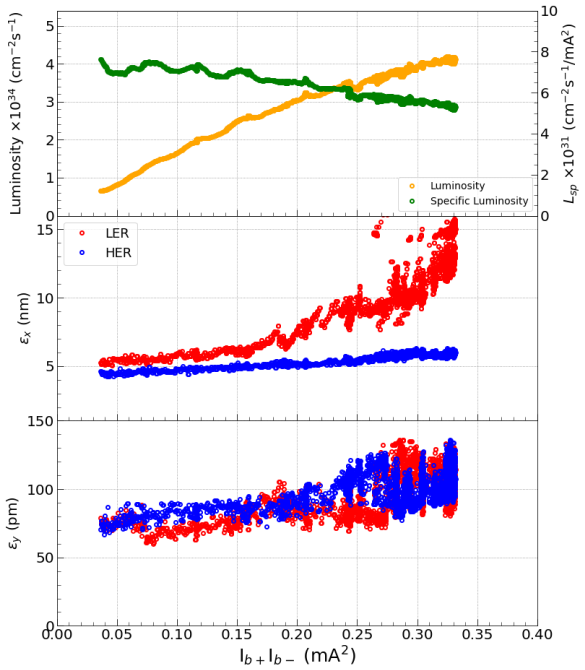

Figure 3: Luminosity and emittance as a function of bunch current product. The β_x^* is 80 mm in the LER.

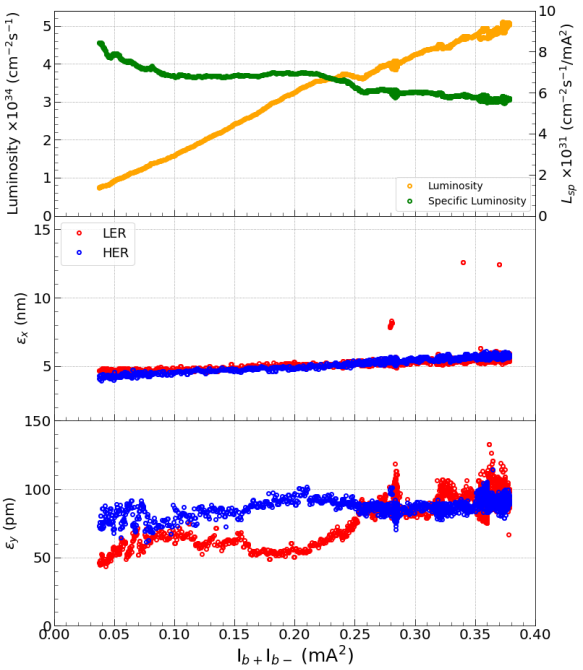

Figure 4: Luminosity and emittance as a function of bunch current product. The β_x^* is 60 mm in the LER.

SBL occurs both in the LER and the HER, however, the event rates in the LER is much higher than that of the HER. A large number of MO-type flanges are used in the LER than in the HER, where they are only used in the interaction region (IR) at SuperKEKB. SBL events have been significantly reduced by cleaning several MO-type flanges. It has been concluded that interactions between the beam and dust particles are the primary cause of SBL events.

Figure 7 shows the vertical beam size measured by the streak camera during an SBL event in the LER. A beam abort caused by an RF cavity breakdown is also shown in the figure. It has been observed that the vertical beam size increases significantly just before the beam abort during SBL events. This behavior is similar to that observed in dust events. The shape of the charged dust distribution resembles that of a flat beam. As a result, the vertical momentum change becomes larger than that in the horizontal direction due to the higher vertical density. While electron clouds generated by ionization and heating quickly disappear, a vertical defocusing effect remains due to the presence of positive ions.

A numerical simulation using the Particle-In-Cell (PIC) method was performed to investigate the interaction between the beam and dust particles [12]. A dust particle undergoes ionization loss, heating, melting, fission, and evaporation. In the case of a dust particle with 50 μm radius, the beam envelope increases more than $50\sigma_y$ in the vertical direction. The vertical beam size is large enough to cause significant beam loss.

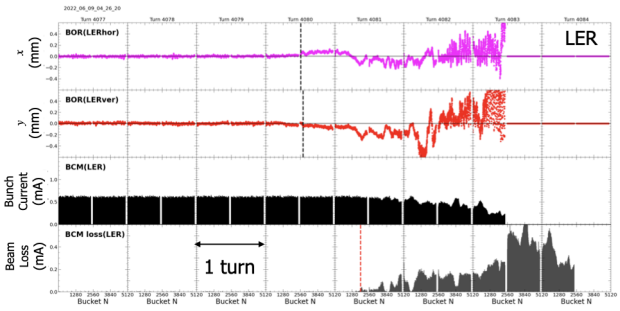

Figure 5: SBL event. Horizontal and vertical position, bunch current of every bunches for 6 turns before beam abort. The amount of beam loss is also indicated.

NONLINEAR COLLIMATOR

Nonlinear collimator [13] was newly installed in one of the straight sections of the LER to mitigate beam backgrounds without increasing impedance. The collimator is placed between a pair of two skew sextupoles to reduce the vertical beam halo. The momentum change in the vertical direction caused by skew sextupoles is written by

$$\Delta p_y = \frac{B_x L}{B\rho} = \frac{K_2}{2}(y^2 - x^2), \tag{10}$$

where K_2 is the magnetic field strength of the skew sextupoles. Either the upper or lower collimator head with a relatively large aperture is used to intercept beam halo particles. The transformation between the skew sextupoles is $-I'$, and the phase advance to the IP is $\pi/2$ in the vertical

Figure 6: VACSEAL as black stains in the MO-type flange connection.

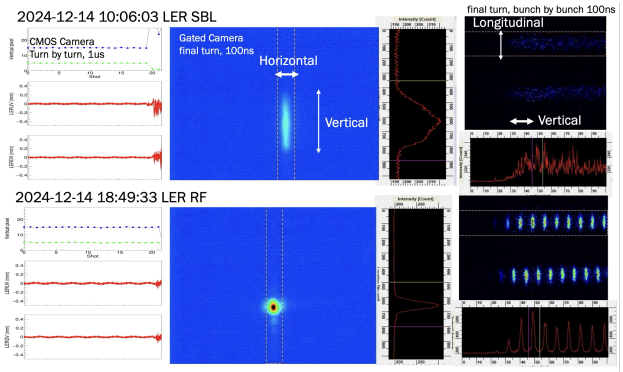

Figure 7: Vertical beam size measured by the streak camera. Upper is a SBL event and lower is a RF breakdown.

direction. During the 2024 spring run, the beta functions at the skew sextupole were $\beta_x = 7$ m and $\beta_y = 378.5$ m. A smaller β_x at the skew sextupoles is effective for eliminating particles with large horizontal amplitudes – particularly those from injection beams. A $\beta_x = 3$ m has been adopted for the 2024 autumn run [14].

MACHINE IMPERFECTION

One of the machine imperfections is a manufacturing defect in the HER cancel coils, which are intended to compensate for the leakage-field from the final focus coils (QC1P) in the LER. This manufacturing defect induces undesired skew sextupole and skew octupole fields in the HER. An effective Hamiltonian [15] is introduced to study nonlinear behavior; in particular, third order terms are described by

$$H_{eff} = \sum_{i,j,k,l\geq 0} C_{ijkl} x^i p_x^j y^k p_y^l, \quad i+j+k+l = 3. \qquad (11)$$

The beam trajectory is different from the nominal beam line. Moreover, the final focus coils have an offset from the nominal beam line axis. A feed-down effect is considered to calculate the effective Hamiltonian. The interaction region ($-4\,m < IP < +4\,m$) [16] is modeled in SAD using 1 cm-thick slices of multipole elements. For each slice, the normal and skew magnetic-field components are

$$\frac{\tilde{K}_p + i\tilde{S}_p}{(p+1)!} = \sum_{n=p}^{\infty} \frac{K_n + iS_p}{(n+1)!} \begin{pmatrix} n+1 \\ p+1 \end{pmatrix} \delta_z^{n-p} e^{-i(n+1)\theta}, \qquad (12)$$

where $\delta_z = z_{cod} - z_{slice}$, $z = x + iy$, and θ is the rotation angle of the slice. An imperfection in the cancel coils enhances specific third-order nonlinear terms. It was found that the contributions from the p_y^3 and $p_x^2 p_y$ terms significantly degrade the luminosity at the higher bunch current product [17], as shown in Fig. 8. The nonlinear terms, p_y^3 and yp_y^2 also reduce a dynamic aperture in the HER.

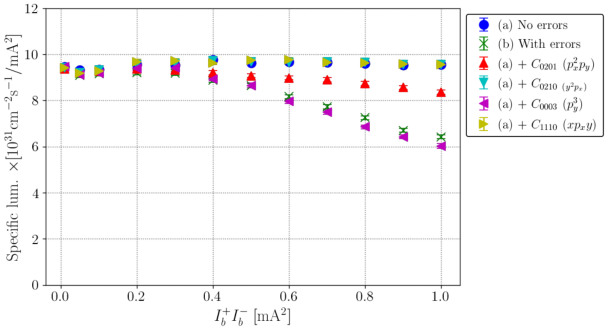

Figure 8: Specific luminosity calculated by Beam-Beam simulations with Weak-Strong model.

OPERATION STATUS

Operation resumed in 2024 following a one-and-a-half-year shutdown (LS1). The operation history since 2019 is shown in Fig. 9. Several major issues remain to be addressed.

- Sudden Beam Loss (SBL)
- Beam-Beam blowup
- Short lifetime and narrow dynamic aperture
- The large emittance of injection beam results in poor injection efficiency [18]
- Deformation of the vacuum pipe due to intense SR heating results in optics deformation caused by orbit offsets at the sextupole magnets [19].

The machine parameters achieved in 2024 and those for a primary target luminosity within a few years are shown in Table 1. In the table, Σ_y^* is the square root of the sum of the squares, σ_{y+}^* and σ_{y-}^*, estimated from the luminosity, and ξ_y is calculated from the luminosity with assuming an equal beam distribution between the LER and HER. From Eqs. (5) and (6), ξ_y is obtained by

$$\xi_{y\pm} = \frac{2er_e}{\gamma_\pm} \frac{\beta_{y\pm}^* L}{I_\pm}. \qquad (13)$$

The peak luminosity of 5.1×10^{34} cm^{-2}s^{-1} is the world highest record. The number of bunches is 2346 which is the design value. The maximum beam current is 1.7 A in the LER and 1.3 A in the HER, respectively. In order to improve the luminosity by increasing higher total beam currents, the bunch current must be increased.

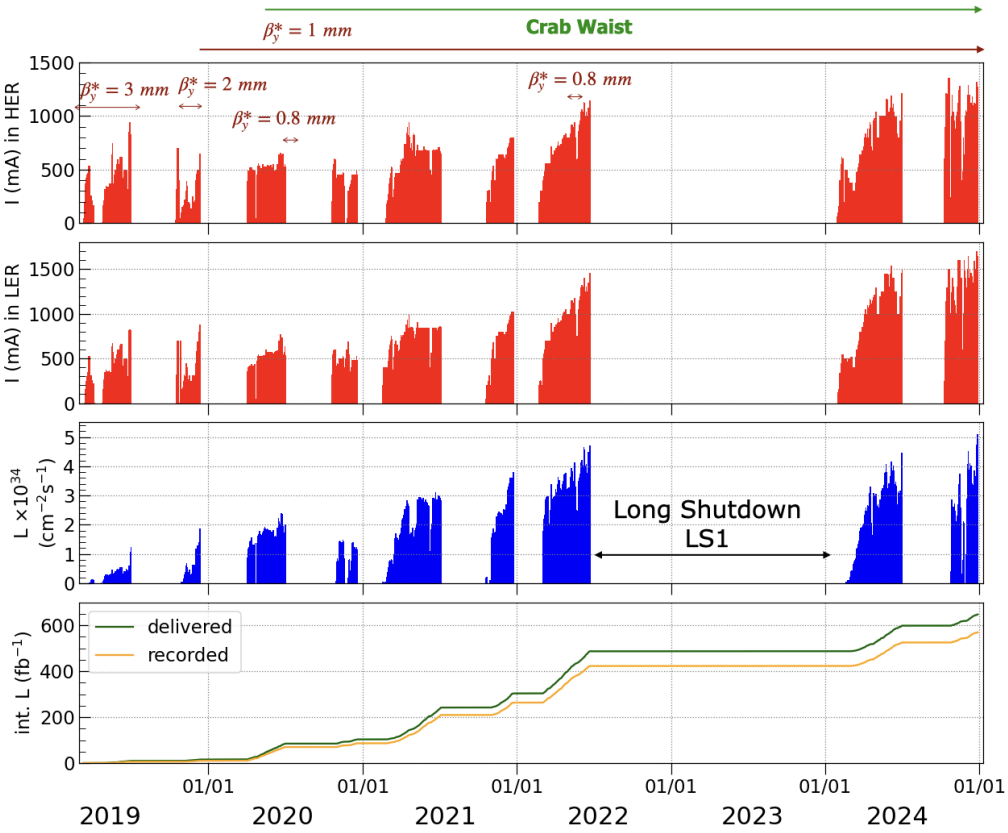

Figure 9: Operation history of SuperKEKB since 2019.

Table 1: Machine Parameters in 2024 and for Primary Target

	Dec. 27 2024		Primary Target	
Ring	**LER**	**HER**	**LER**	**HER**
ε_x (nm)	4.0	4.6	4.0	4.6
I (mA)	1632	1259	2080	1480
n_b	2346		2346	
I_b (mA)	0.696	0.537	0.89	0.63
σ_x^* (μm)	15.5	16.6	15.5	16.6
Σ_y^* (μm)	0.375		0.217	
β_x^* (mm)	60	60	60	60
β_y^* (mm)	1.0	1.0	0.8	0.8
ν_x	44.525	45.531	44.525	45.532
ν_y	46.589	43.599	46.589	43.573
ν_s	0.024	0.027	0.024	0.027
σ_z (mm)	4.6(6.0)	5.1(6.1)	4.6(6.5)	5.1(6.4)
Φ	12.3	12.7	12.3	12.7
R_{cw} (%)	80	60	80	80
ξ_y	0.036	0.027	0.044	0.036
L (cm^{-2}s^{-1})	5.1×10^{34}		10^{35}	

CONCLUSION

The machine operation resumed in 2024 after the LS1. The highest peak luminosity of 5.1×10^{34} cm^{-2}s^{-1} was achieved without data taking by the Belle II detector. If sudden beam loss (SBL) is caused by beam-dust interactions originating from amorphous graphite formed from VACSEAL inside MO-type flanges, cleaning is expected to reduce the frequency of SBL events. Beam-Beam blowup remains a serious issue. The vertical emittance increases with the bunch current product, even though it remains at a level of 20 pm on the single beam (i.e., without collision). The crab-waist scheme helps improve luminosity performance; however, its effect is not perfect. Optics with β_y^* = 1 mm in both rings and β_x^* = 60 mm in the HER were adopted. In the LER, β_x^* = 80 mm optics had previously been applied, but horizontal emittance blowup was observed at the bunch current product increased. After squeezing β_x^* from 80 mm to 60 mm in the LER, no horizontal emittance blowup has been observed. Synchro-beta and betatron resonances significantly affect luminosity performance. Combined effects of beam-beam interactions, lattice nonlinear, and wakefield should be considered to accurately evaluate luminosity performance. Beam-Beam simulations using the Strong-Strong model with the actual lattice are currently being performed on GPU machines.

REFERENCES

[1] R. T. Garcia *et al.*, "Smallest vertical beam sizes achieved in high-energy accelerators", Jun. 2025, arXiv:2506.12361 [physics.acc-ph]. doi:10.48550/arXiv.2506.12361

[2] *SuperB Conceptual Design Report*, INFN/AE-07/2, SLAC-R-856, LAL 07-15 Mar. 2007.

[3] K. Oide *et al.*, "Design of beam optics for the future circular collider e+e− collider rings",*Phys. Rev. Accel. Beams*, vol. 19, p. 111005, 2016. doi:10.1103/PhysRevAccelBeams.19.111005

[4] M. Zobov *et al.*, "Test of "crab-waist" collisions at the DA NE factory", *Phys. Rev. Lett.*, vol. 104, p. 174801, 2010. doi:10.1103/PhysRevLett.104.174801

[5] D. Shatilov *et al.*, "Application of frequency map analysis to beam-beam effects study in crab waist collision scheme", *Phys. Rev. ST Accel. Beams*, vol. 14, p. 014001, 2011. doi:10.1103/PhysRevSTAB.14.014001

[6] D. Zhou *et al.*, "Simulations and experimental results of beam-beam effects in SuperKEKB", *Phys. Rev. Accel. Beams*, vol. 26, p. 071001, 2023. doi:10.1103/PhysRevAccelBeams.26.071001

[7] Y. Ohnishi *et al.*, "SuperKEKB operation using crab waist collision scheme", *Eur. Phys. J. Plus*, vol. 136, p. 1023, 2021. doi:10.1140/epjp/s13360-021-01979-8

[8] K. Ohmi, "Strong-strong Simulation for Super B Factories", in *Proc. IPAC'10*, Kyoto, Japan, May 2010, paper TUPEB013, pp. 1542–1544.

[9] H. Ikeda *et al.*,"Observation of sudden beam loss in SuperKEKB", *in Proc. IPAC2023*, Venice, Italy, May 7-12, 2023. pp. 716–719. doi:10.18429/JACoW-IPAC2023-MOPL072

[10] M. Tobiyama and J. W. Flanagan, "Development of bunch current and oscillation recorder for SuperKEKB accelerator", in *Proc. IBIC2012*, Tsukuba, Japan, Oct. 2012, paper MOPA36, pp. 138–142. https://jacow.org//IBIC2012/papers/MOPA36.pdf

[11] K. Shibata *et al.*, "Sudden Beam Loss (SBL) events at SuperKEKB, observations and measures", presented at eeFACT2025, Tsukuba, Japan, Mar. 2025, Paper FRA07. https://indico.jacow.org/event/75/contributions/7096/.

[12] K. Ohmi *et al.*, "Simulations on SBL", presented at eeFACT2025, Tsukuba, Japan, Mar. 2025, Paper FRA08. https://indico.jacow.org/event/75/contributions/7097/.

[13] N. Merminga *et al.*, "Optimizing a nonlinear collimation system for future linear colliders", in *Proc. PAC'91*, San Francisco, CA, USA, May 1991, pp. 219–222.

[14] S. Terui *et al.*, "Collimator challenges at SuperKEKB and their countermeasures using nonlinear collimator", *Phys. Rev. Accel. Beams*, vol. 27, p. 081001, 2024. doi:10.1103/PhysRevAccelBeams.27.081001

[15] K. Hirosawa *et al.*, "The influence of higher order multipoles of IR magnets on luminosity for SuperKEKB", in *Proc. IPAC2018*, Vancouver, BC, Canada, Apr. - May 2018. doi:10.18429/JaCow-IPAC2018-THPAK099

[16] N. Ohuchi *et al.*, "SuperKEKB beam final focus superconducting magnet system", *Nucl. Inst. Meth. A* vol. 1021, p. 165930, Oct. 2021. doi:10.1016/j.nima.2021.165930

[17] H. Sugimoto, private communications.

[18] N. Iida *et al.*, "SuperKEKB injector and injection (status and progress)", presented at eeFACT2025, Tsukuba, Japan, Mar. 2025, Paper TUB01. https://indico.jacow.org/event/75/contributions/6798/.

[19] H. Sugimoto *et al.*, "Beam optics distortion caused by orbit deviation at strong sextupole magnets in SuperKEKB", *JINST* vol. 19, p. P02012, Feb. 2024. doi:10.1088/1748-0221/19/02/P02012